Accepted Manuscript

A Theoretical Model to Estimate Inactivation Effects of OH radicals on Marine *Vibrio* sp. in Bubble-Shock Interaction

Y. Huang, J. Wang, A. Abe, Y. Wang, T. Du, C. Huang

PII: S1350-4177(18)30880-0
DOI: https://doi.org/10.1016/j.ultsonch.2018.10.001
Reference: ULTSON 4334

To appear in: *Ultrasonics Sonochemistry*

Received Date: 7 June 2018
Revised Date: 7 September 2018
Accepted Date: 2 October 2018

Please cite this article as: Y. Huang, J. Wang, A. Abe, Y. Wang, T. Du, C. Huang, A Theoretical Model to Estimate Inactivation Effects of OH radicals on Marine *Vibrio* sp. in Bubble-Shock Interaction, *Ultrasonics Sonochemistry* (2018), doi: https://doi.org/10.1016/j.ultsonch.2018.10.001

This is a PDF file of an unedited manuscript that has been accepted for publication. As a service to our customers we are providing this early version of the manuscript. The manuscript will undergo copyediting, typesetting, and review of the resulting proof before it is published in its final form. Please note that during the production process errors may be discovered which could affect the content, and all legal disclaimers that apply to the journal pertain.

ACCEPTED MANUSCRIPT

A Theoretical Model to Estimate Inactivation Effects of OH radicals on Marine *Vibrio* sp. in Bubble-Shock Interaction

Y. Huang [(1)(4)], J. Wang*[(1)(2)], A. Abe [(3)], Y. Wang *[(1)(2)], T. Du [(1)(2)], C. Huang [(1)(2)]

(1) Key Laboratory for Mechanics in Fluid Solid Coupling System, Institute of Mechanics, Chinese Academy of Sciences, No.15 Beisihuanxi Road, Beijing, 100190, China

(2) School of Engineering Science, University of Chinese Academy of Sciences, Beijing, 100049, China

(3) Graduate School of Maritime Sciences, Kobe University, 5-1-1 Fukaeminami-machi, Kobe, 658-0022, Japan

(4) High School Affiliated to Renmin University of China, Beijing, 100080, China

* Corresponding Author's email: wangjingzhu@imech.ac.cn and wangyw@imech.ac.cn

Abstract

A theoretical model for estimating inactivation effects on marine *Vibrio* sp. is developed from the viewpoint of the chemical action of the OH radicals induced by interaction of bubbles with shock waves. It consists of a biological probability model for cell viability and a bubble dynamic model for its collapsing motion due to the shock pressures. The biological probability model is built by defining a sterilized space of the OH radicals. To determine the radius of the sterilized space, the Herring equation is solved in the bubble dynamic model in consideration of the effect of the heat conductivity and mass transportation. Furthermore, the pressure waveform of incident shock wave used in the model is obtained with the pressure measurement. On the other hand, a bio-experiment of marine *Vibrio* sp. is carried out using a high-voltage power supply in a cylindrical water chamber. Finally, the viability ratio of marine bacteria estimated by the theoretical model is examined under the experimental conditions of this study. In addition, we also discuss the influence of bubble initial size for predicting the inactivation effects.

Key Words: Theoretical model, Bubble-shock interaction, Chemical inactivation, Biological probability model, Generation and diffusion of OH radicals

1. Introduction

The bubble dynamics have been studied in detail experimentally, theoretically, and numerically. After exposed to a pulse of pressure, bubbles oscillate and collapse with physical and chemical phenomena. Some destructive productions such as strong pressure pulse, high-speed jet, and oxidative free radicals are generated so that the tissues and cells around them would be damaged by their mechanical and biochemical actions. Takayama [1] found the collapsing motion of cavitation bubbles could result in the tissue damage of the body when they tried to employ underwater shock wave focusing in an ellipsoidal reflector to develop an extracorporeal shock wave lithotripsy. Delius et al. [2] examined the effects of shock wave-gas bubble interaction on cell destruction at the minimum static excess pressures. The freed hemoglobin was identified as a marker of cell destruction. They noted that shock waves with the amplitude of 400 kPa caused membrane destruction and other biological effects. Lokhandwalla and Sturtevant [3] analyzed the interactions of red blood cells with shock-induced shear flow and bubble-induced radial flow fields in a shock wave lithotripsy, respectively. They found that the extensional fluid motion induced by both of the flow fields contributed mainly to the cell deformation and a tension in the cell membrane [4]. Loske et al. [5] investigated the bactericidal effect of *Escherichia coli* in an electrohydraulic shock wave generator in order to develop a non-thermal food preservation method using shock waves. And they indicated that the bacteria were inactivated by the mechanical action of the shock wave. Okada et al. [6] used single-shot pulsed ultrasound to investigate the respective contributions of mechanical effect and sonochemical effect on cell membrane damages. Their results showed that the damage of cell membrane adjacent to microbubbles was mainly caused by mechanical effect rather than sonochemical effects.

For its application to marine sciences, Abe et al. [7] proposed a shock wave sterilization method for killing marine bacteria in a ship's ballast water using the collapse of bubbles induced by incident shock waves. In the sterilization method, the products like rebound shock waves and free radicals are expected to inactivate marine bacteria by their mechanical and biochemical actions. They investigated the cell damage induced by the shock wave pressure via an electron microscope. The cell was regularly deformed by the shock pressure. It differed from the irregular deformation by the osmotic pressure. Furthermore, they examined the tolerance of marine *Vibrio* sp. to the shock pressure by using a gas gun [8] and measured the pressure pulse emitted from the collapse of microbubble [9]. These results indicated that rebound shock waves generated by the bubble motion had a potential to kill marine bacteria. Wang and Abe [10] carried out a bio-experiment of marine *Vibrio* sp. to clarify the sterilization effects of this method in a circular-flow water tank. Furthermore, they also examined the respective effect of mechanical action and biochemical action by adding sodium L-ascorbate to the cell suspension. The results showed that free radicals mainly contributed to inactivating marine bacteria in their experimental condition [11]. Based on the theoretical and experimental studies [12-17], these free radicals are the products of chemical reactions inside a bubble. As a result of bubble collapse, the internal temperature and pressure reach thousands of absolute temperature and hundreds of atmospheres or more, so that water vapor and non-condensable gas inside the bubble are dissociated. Free radicals generated by the bubble motion, hydroxyl (OH) radicals, have extremely high oxidization, so that they are dominant to sterilization of marine bacteria. For investigating inactivation effects of OH radicals, Bai et al. [18] used a physical method of strong electric-field discharge to generate the OH radicals. The results showed that it was effective to apply the OH radicals for killing marine bacteria and algae in ships' ballast water.

ACCEPTED MANUSCRIPT

ACCEPTED MANUSCRIPT

On the other research, Sundaram et al. [19] proposed a theoretical model to relate the membrane permeabilization to the number of transient cavitation event when they investigated the viability of cells exposed to varying does of acoustic energy using a suspension of 3T3 mouse cells. They suggested that the critical strains of the membranes could be easily exceeded when the cells were exposed to microbubble-induced shock waves. Given the mechanisms of cell disruption by shear forces, a simple model was developed to investigate the inactivation ratio of Enterobacter aerogenes under low-frequency high-power ultrasound in the study of Gao et al. [20]. The fits obtained with the model were in good agreement with the experimental data. Wang and Abe [21] built a hybrid analytical model to estimate sterilization effects considering the inactivation both free radicals and collapsing shock waves. The sterilized space was assumed where the pressure behind the rebound shock wave front was stronger than 150 MPa, and their estimation was consistent with the experimental results. Based on their study, we also develop a theoretical model to estimate inactivation effects of the OH radicals generated by bubble-shock interaction in the present study. The present theoretical model consists of a biological probability model for cell viability and a single bubble dynamic model for the interaction of bubbles with shock waves. In the bubble dynamic model, the transfer of the heat and mass through the boundary interface between bubble and water are considered to determine temperature condition for the generation of the OH radicals. The pressure waveform of incident shock wave used in the model is attained by the pressure measurement. On the other hand, the validity of the theoretical model is made by comparison with a bio-experiment of marine *Vibrio* sp.. Finally, the viability ratio of marine bacteria obtained with the theoretical model is examined under the experimental conditions of this study. In addition, we also discuss the influence of bubble initial size for predicting the inactivation effects.

2. Bio-experimental setup

Figure 1 shows a bio-experimental arrangement for investigating sterilization effects. The experimental system consisted of a cylindrical water chamber, a high-voltage power supply (HPS 18K-A, Tamaoki Electronics Co-Ltd), and a pulse generator. The external dimension of the cylindrical water chamber was 90 mm in diameter and 120 mm in length. There were two equivalent parts, namely, the upper part was a test chamber and the lower was an electric discharge chamber. The shape of each part was a cylinder of 30 mm in diameter and 30 mm in depth with a circular cone of a 30-mm diameter, and depth of the taper end was 6 mm. A 0.1-mm silicone film was used to separate the two parts. Two parallel slots in the electric discharge chamber were equipped for the installation of electrodes. A slot with a 6.5-mm diameter at the top of the test chamber was designed for the setup of a probe of pressure transducer and for the sample extraction of cell suspension. Given the mechanism of underwater electric discharge, incident shock waves are generated by the expansion of the thermal plasma channel consisting of high-temperature vapor. Next, a vapor bubble is formed at the tips of the two electrodes. As described in our previous study [11], with the expansion and contraction of the vapor bubble, the oscillation of the silicone-film separator is caused, and then resulting in the up-and-down movement of the liquid surface in the slot of test chamber. Consequently, air in the slot is brought rapidly into the water chamber and simultaneously an increasing number of the bubbles are generated in this way. These bubbles still remain when the next incident shock wave is coming. The collapses of these air bubbles take mainly responsibility for the inactivation of marine bacteria due to number density and long lifetime of air bubbles [11]. In addition, the UV produced by the electric discharges has no inactivation effects on marine bacteria, as described in Appendix.

In the experiments, incident underwater shock waves were generated with the frequency of 1 Hz, i.e., the electric discharge was triggered once every second. The output power was 31.6 kV. The electric discharge chamber and the test chamber were filled with the distilled water and the cell suspension of marine *Vibrio* sp., respectively. Furthermore, the upper end of the slot in the test chamber was covered with a rigid wall during the experiment. Here, samples of 0.1 ml were extracted regularly from the cell suspension, diluted serially, and then spread on agar plates. The plates were incubated for 24 hours at 35 ℃. Finally, the cell viability in 1 ml was evaluated using the numbers of colony-forming cells on the agar plates on the basis of the dilution ratio, as shown in Fig. 2.

3. Theoretical model for estimating sterilization effect

3.1 Biological probability model

In the previous studies on the inactivation of marine *Vibrio* sp. using bubble-shock interaction, the results showing the contribution of OH radical has been obtained [11]. Extremely high-temperature and pressure are required to break up chemical bonds of H_2O and gasses in order to produce the OH radicals. In the bubble-shock interaction, an influence area of high-temperature may be confined inside and in the vicinity of the bubble surface since the temperature at the bubble-water interface basically equals to the water temperature [22]. Consequently, it is thought that most of the OH radicals are generated inside the bubble and transferred into water [23-27]. Therefore, the OH radicals dissolving into water probably just exist in a thin layer of bubble-water interface [28, 29]. The space in which the marine bacteria will be strongly affected by the OH radicals is defined as the sterilized space in the biological probability model. Figure 3 is a schematic of the sterilized space of a single bubble from the test chamber filled with the cell suspension. It is assumed that the number of microbubbles M and the number of marine bacteria N_0 randomly distribute in the test chamber with a volume of V, and then the water volume and the number of marine bacteria for

ACCEPTED MANUSCRIPT

a single bubble are V_b and N_b, respectively. The sterilized space is represented as a sphere of radius, r_s including the interior of the bubble.

We consider the cell viability of marine bacteria after an incident shock wave passes though M of the bubbles in the test chamber. First of all, as shown in Fig. 3 (b), the number of inactivated bacteria around one bubble, in other words, the number of bacteria located in the sterilized space, N_s, is given by

$$N_S = \frac{4}{3}\pi r_s^3 \frac{N_b}{V_b}, \quad (1)$$

where these bacteria of N_b is assumed to distribute randomly in the water volume of V_b regardless of the position of the bubble since there is possibility that the bacteria exist inside the bubble owing to their small sizes. The water volume $V_b = V/M$ and the number of bacteria $N_b = N_0/M$ for a bubble are obtained.

Therefore, the cell viability ratio of the bacteria after the collapse of one bubble, α_1, is expressed as follows:

$$\alpha_1 = 1 - \lambda_1, \quad (2)$$

$$\lambda_1 = N_S/N_b = \frac{4}{3}\pi r_s^3 \frac{1}{V_b}, \quad (3)$$

where the subscript 1 means the number of the bubbles generated in the test chamber. The inactivation ratio of the bacteria λ is presumed to the same for every bubble, i.e., $\lambda_1 = \lambda_2 = \ldots\ldots = \lambda_M$ in the model.

Next, given that the distribution of microbubbles and bacteria in the cell suspension of the test chamber is random, the cell viability ratio after M of bubbles collapse, α_M, is given by

$$\alpha_M = 1 - \frac{\lambda_1}{M}\sum_{m=1}^{M}(1-\lambda_1)^{M-1}. \quad (4)$$

After a Taylor expansion, Eq. (4) can be rewritten as

$$\alpha_M \approx e^{-\lambda_1}. \quad (5)$$

The number of viable cells for once incidence of shock wave, is presented by,

$$N_1 = \alpha_M \times N_0. \quad (6)$$

Finally, the bacteria viability ratio after t-shot incidences of shock waves, is shown as follows:

$$\frac{N_t}{N_0} = {\alpha_M}^t = e^{-\lambda_1 t}. \quad (7)$$

Hence, the bacteria viability ratio is determined by two parameters, λ_1 and t, where λ_1 depends on the radius of the sterilized space r_s around a bubble and the number of the bubbles M in the test chamber, and t is related to the number of the electric discharges.

3.2 Bubble dynamic model

To obtain the value of λ_1 in Eq. (3), it requires to obtain the radius of the sterilized space, r_s, relative to the generation condition of the OH radicals. It is difficult to directly measure or observe the generation of the OH radicals due to their fast reactions in a dynamic stimulus [30]. Few experimental data are available on the concentration of the OH radicals for a single air bubble in water. In the present paper, a bubble dynamic model was developed to analyze the generation and diffusion conditions of the OH radicals. Its schematic is shown in Fig. 4. The bubble begins to contract just after exposed to the pressure of incident shock wave. The chemical and physical phenomena, such as a luminescence flash called as sonoluminescence are caused with increasing the internal temperature and pressure [31, 32]. Zhang et al. [33] argued that the luminescence flash occurred at tens of microseconds before the bubble reached the minimum size. These results indicate that thermal decomposition of the gas molecules can occur before the temperature reaches the peak. In other researches, Locke et al. [34] used a planar laser-induced fluorescence method to investigate a large-scale and high-pressure combustor environment and obtained the images of the OH radicals at the inlet of 1034 kPa and 866 K. Varatharajan and Williams [35] investigated the high-temperature oxidation of acetylene numerically and theoretically, and reported that the OH radicals were formed by the reaction of the H radicals and O_2 under the initial condition of 50 bar and 1100 K. The study by Abe et al. [9] also found that free radicals were generated after the passage of underwater shock waves with amplitude of about 200 MPa at 293 K when they used a gas gun to investigate the tolerance of marine *Vibrio* sp. against the shock pressure. Consequently, it is suggested that the conditions to generate the OH radicals are related closely to the experimental conditions. In the previous study [11], the OH radicals are suggested to be generated at about1000 K of internal temperature in the interaction of air bubbles with underwater shock waves. Based on these backgrounds, we define a 1000-K temperature as critical condition for the generation of the OH radicals in the model.

As shown in Fig. 4 (b), a thermal boundary layer with a temperature drop is basically formed in the gas inside the bubble since the density and specific heat of water are so much larger than the respective values for gas. It is assumed the temperature is spatially uniform at the center of the bubble, while to be linear within the boundary layer. Therefore, the radius of the sterilized space, r_s, is defined as the bubble radius when internal temperature becomes

ACCEPTED MANUSCRIPT

over 1000 K. For the diffusion of the OH radicals, the diffusion constant is approximately equal to the thermal conductivity given the study of Toegel et al. [36]. As a result, the heat and mass are suggested to transfer through the same boundary layer. According to the generation mechanism of the bubble in the cylindrical water chamber, the bubble is assumed to be filled with ideal gas, air. Therefore, most of the OH radicals are generated by thermal decomposition of water vapor. To simply the bubble dynamic model, the OH radicals are assumed to transfer to the outside with the mass transportation of water vapor through the boundary layer. In addition, the gas inside the bubble except water vapor are thought to be noble gas.

In the model, we applied the Herring bubble motion equation [37] to analysis of interaction between a bubble and an underwater shock wave, as shown in Eq. (8),

$$\left(1-\frac{2\dot{R}}{C_\infty}\right)R\ddot{R}+\frac{3}{2}\left(1-\frac{4}{3C_\infty}\dot{R}\right)\dot{R}^2+\frac{1}{\rho_\infty}\left(P_\infty-P_s-\frac{R}{C_\infty}\frac{dP_s}{dt}\right)=0 \quad (8)$$

where R is the bubble radius, $\dot{R}$ = dR/dt, t is the time, $\ddot{R}$ = d$\dot{R}$ /dt. C_∞ is the sound speed of water at infinity, ρ_∞ is the density of water at infinity, and P_s is the pressure at the interface of a bubble, P_∞ is the pressure behind an external incident shock wave inducing the collapse of bubble.

C_∞ is given by,

$$C_\infty=\sqrt{\frac{n(P_\infty+B)}{\rho_\infty}}, \quad (9)$$

where B and n are constant values, B = 2963 bar and n = 7.41.

P_s is described by,

$$P_s=P_{in}-\frac{1}{R}(2\sigma+4\mu\dot{R}), \quad (10)$$

where σ is the surface tension, and μ is the viscosity coefficient, and P_{in} is the pressure of the gas inside the bubble.

An ideal gas equation was used as,

$$P_{in}v=R_gT_{in}, \quad (11)$$

where v and T_{in} are the molar volume and temperature of the gas inside the bubble, and R_g = 8.3145 J/(mol K). The molar volume v is presented by

$$v=\frac{N_AV}{N_{Tot}}, \quad (12)$$

where N_A is the Avogadro number, 6.02×10^{23}, the volume of the bubble $V=4/3\pi R^3$, and N_{Tot} is the total number of gas molecules in the bubble, consisting of the number of water vapor N_{water} and other molecules N_{others},

$$N_{Tot}=N_{water}+N_{others}. \quad (13)$$

In the model, the gas except water vapor inside the bubble was presumed not to involve in the mass transportation. During the bubble motion, the rate of particle changes for water vapor [38] can be estimated by Eq. (14)

$$\dot{N}_{water}\approx 4\pi R^2D\frac{C_r-C}{l_{diff}}, \quad (14)$$

where C_r=C_r (T_0) corresponds to the equilibrium density at the wall [39, 40], $C_r = P_v(T_0)/kT_0 \approx 5.9\times10^{23}$ m^{-3} for T_0=293.15K, k is the constant, 1.38×10^{-23} [36], C is the actual concentration of water vapor inside the bubble, $C = N_{water}/V$, D is the diffusion constant. As mentioned above, we obtained the diffusive penetration depth, $l_{diff}\approx\delta$, the thickness of thermal boundary layer. Hence, the instantaneous diffusive penetration depth l_{diff} can be expressed by the Rayleigh-Plesset time τ_c [11, 41], referring to the calculation of thermal boundary.

$$l_{diff}=\sqrt{\alpha_g\tau_c}=\sqrt{(\lambda_g/\rho_gC_p)0.915R_0\sqrt{\frac{\rho_l}{\Delta P}}}, \quad (15)$$

where λ_g is the thermal conductivity, C_p the heat capacity at constant pressure, ρ_g is the density of gas, ΔP is the difference pressure between outside and inside the bubble.

Considering the effect of the thermal conductivity at the bubble wall, the energy balance of the gas inside the bubble is written in Eq. (16) according to the first law of the thermodynamics for an open system,

$$\dot{E}=h\dot{N}_{water}+\dot{Q}-\dot{W}, \quad (16)$$

ACCEPTED MANUSCRIPT

where h denotes the enthalpy per water molecule, $h \approx 8/2kT_0$, Q is the heat transfer to the bubble, W represents the work done by the bubble, and dots on the upper side denotes the differential of the variables. In addition, the heat of reaction occurring inside the bubble is neglected in the system according to the studies in Refs. [42-45]

The internal energy is made up of the translation energy of the molecule of gas and the internal energy of the molecule of water vapor [36].

$$E = \frac{3}{2}N_{others}kT + \left[\frac{6}{2} + \sum\left(\frac{\theta_{i/T}}{e^{\theta_{i/T}} - 1}\right)\right]N_{water}kT, \quad (17)$$

where θ_i are the characteristic vibrational temperatures, $\theta_1 = 2295$ K, $\theta_2 = 5255$ K, and $\theta_3 = 5400$ K [36].

According to the Fourier's law, the heat loss ΔQ through the thermal boundary layer can be written in Eq. (18).

$$\Delta Q \approx \frac{\lambda_g(4\pi R^2)\Delta T}{\delta}\Delta t = \frac{\lambda_g(4\pi R^2)(T_0 - T_{in})}{\delta}\Delta t. \quad (18)$$

Where δ is the thickness of the boundary layer, $\delta \approx l_{\text{diff}}$.

The work one by the bubble is describe by Eq. (19),

$$\dot{W} = P_s\dot{V}\,. \quad (19)$$

Finally, the Herring bubble motion equation (8) was solved using the fourth-order accurate Runge-Kutta-Gill method. Then, from Eqs. (10), (11), and (12), the pressure changes at the interface, dP_s/dt, is derived as the following equation;

$$\frac{dP_s}{dt} = \left(\frac{R_g N_{Tot}}{N_A V}\dot{T} + \frac{R_g T}{N_A V}\dot{N}_{Tot} - \frac{R_g T N_{Tot}\dot{V}}{N_A \quad V^2}\right) + \frac{1}{R^2}\left(2\sigma\dot{R} + 4\mu\dot{R}^2 - 4\mu\ddot{R}R\right). \quad (20)$$

3. Results and discussion

Figure 5 shows the estimation on the cell viability at 31.6-kV electric discharges in the test chamber. The electric discharge was triggered once every second, i.e., the applied frequency of incident shock waves was 1 Hz. An air gap of 10 mm in the slot was set to make the water surface move freely, so that numerous bubbles were generated. In the experiments, the height of the air gap was maintained by putting an equivalent amount of artificial seawater into the cell suspension after every sample extraction. The effect of the artificial seawater on the dilution of the cell suspension was removed when sterilization effects were estimated. The initial density of marine bacteria was about 4.62×10^6 cfu/ml. The solid diamonds in the figure are of the average for 6 sets of bio-experimental data. Here, the error bars are not shown because the low value of the standard deviation (STD) are not clearly recognized in the exponentially ordinate of the viability ratio. In the figures including the following bio-experimental results, the STD are less than 15, even close to 0 except the point (STD $\approx$ 27) at the beginning of the experiments. Samples were taken from the test chamber every 20-shot electric discharges after the beginning of the bio-experiment. In the experiments, the sodium L-ascorbate was also added in the cell suspension to get rid of the chemical inactivation effects. The results are indicated by the solid squares. The number of marine bacteria hardly change throughout the experiments. It suggests that the mechanical action of the bubble motion take no responsible for killing marine bacteria, and the OH radicals contribute mainly to the activation. From the results without the sodium L-ascorbate as indicated by the solid diamonds, it is found that the viability ratio of marine bacteria is decreasing exponentially and all of marine bacteria are killed completely in about 160 seconds. The results suggest that the strength of the collapsing bubbles keep consistent after every sample extraction. The pressure of incident shock wave is thought to be constant during the experiments. Hence, the number density of the generated bubbles is constant with the extractions of the samples.

To investigate the propagation behaviors of the shock waves in the test chamber, pressure measurements were also carried out using a transducer (Fiber Optical Probe Hydrophone: FOPH 2000, RP acoustic). Figure 6 shows a pressure profile at a 30-mm position of the central axis of the test chamber from the discharge pint obtained with FOPH 2000. In the figure, the experimental data within 10 μs is affected by the light noise of the discharge flash. We observe the 1st shock wave (1st SW) at about 19 μs and the 2nd shock wave (2nd SW) at about 27 μs, respectively. The 1st SW is generated by the electric discharge, and reflected at the inner wall, and concentrate at the central axis of the cylindrical chamber to form the 2nd SW. Based on propagation velocity of underwater shock wave, about 1500 m/s, the 3rd shock wave (3rd SW) is the reflections wave of the 1st SW at the bottom boundary of the electric discharge chamber. There are some expansion regions observed behind the 2nd SW and around the 3rd SW. Cavitation bubbles are thought to be produced in these regions, so that the pressure variation after 30 μs is affected by their collapses. However, the activation effects are barely induced by the motion of these cavitation bubble due to their small number in the present study, compared with the air bubbles generated by the rapid up-and-down movement of liquid surface in the test chamber.

By 20-set pressure measurements at the positions of 20 mm, 30 mm, 40 mm, and 50 mm from the discharge point, the physical characteristics of the 1st shock wave front were obtained. The full width of half maximum (FWHM) was about 0.8 μs, the mean peak was about 4.5 MPa, the rising time to peak pressure was 0.4 μs, and the falling time to

ACCEPTED MANUSCRIPT

atmosphere was about 0.6 μs. Such a pressure waveform of incident shock wave was applied to investigation of the bubble motion in the bubble dynamic model. The other values of the pressures equal to the atmosphere in the profile.

Figure 7 shows analytical results of bubble motion equation substituted by a pressure wave. The initial radius of the bubble took about 50 μm based on the optical images in Ref. [11]. In this analysis, the density of water ρ_∞ = 999.7 kg/m^3, the viscosity coefficient μ = 1.307 × 10^{-3} Pa·s, the surface tension σ = 74 × 10^{-3} N/m, the density of gas ρ_g = 1.20 kg/m^3 at T_0 = 293.15 K when $R = R_0$, the thermal conductivity in the gas λ_g = 0.599 W/(m·K), the heat capacity of gas C_p = 4186 J/(kg·K) , the atmospheric pressure P_0 =1.01325 × 10^5 Pa were used. Figure 7 (a) represents the time variation of radius and pressure of incident shock wave. After the bubble is exposed to the shock pressure, the radius begins to contract and eventually reaches a minimum, about 11.5 μm at about 1 μs, and simultaneously the pressure inside it increases to maximum. After that, the bubble expands to about 104.0 μm since the exposed pressure decrease to the atmosphere, so that a large pressure difference between inside and outside the bubble is caused. Figure 7 (b) shows the time variation of temperature inside the bubble. In the bubble dynamic model, the radius of the sterilized space is defined as the bubble radius when the internal temperature achieves 1000 K. From this figure, we could see that the temperature firstly reaches about 1000 K at t_c = 0.844 μs when the bubble contracts to 25.75 μm and achieves a peak of about 4800 K at the minimum size of the bubble. After that, the temperature decreases with its expansion and secondly reaches about 1000 K when t_e = 1.083 μs and R = 24.79 μm. At the second rebound, the peak internal temperature change to about 1200 K due to the loss of energy induced by the water compressibility, heat conductivity, and mass transportation. Hence, it could be seen that the effective inactivation of marine bacteria is limited to the first rebound of the bubble motion. During the motion of its first rebound, the period to maintain a 1000-K temperature is about 0.24 μs. However, in consideration of high oxidation reaction of the OH radicals, the bacteria would be inactivated just once the radicals are generated, so that we ignore the inactivation time of the radicals and focus on the space distribution of inactivated bacteria for a bubble collapse in the theoretical model. Therefore, the radius of the sterilized space is determined based on the temperature distribution inside and outside the bubble at t_c = 0.844 μs, also presented in the figure. The temperature around the bubble center maintains 1000.23 K and drops linearly to 293.15 of water temperature within the boundary layer. Consequently, the radius of the sterilized space r_s is about 24.46 μm in the theoretical model.

Figure 8 shows the time variation of the number of the total molecules and water vapor inside the bubble. The initial total number of the molecules inside the bubble was determined by Eqs. (11) and (12) when P_{in} = 1.03 × 10^5 Pa, T_{in} = 293.15 K, R = 50 μm. The initial number of water vapor corresponded to the equilibrium density at the wall, C_r. The difference between the number of total molecules and water vapor was defined as the number of other molecules, N_{other}. During the collapse of the bubble, other molecules would not involve in the mass transportation in the bubble dynamic model. As shown in this figure, water vapor diffuses into the outside during its contraction and enters the bubble during its expansion. The minimum and maximum of the water-vapor number are 3.7 × 10^9 and 2.7 × 10^{12}, respectively. Compared with the total number of the molecules, it can be seen that the transfer of the water vapor through the boundary layer has little effects on the mass transportation. Therefore, it is reasonable that the characteristics of the gas inside the bubble keep consistent with that of air, so that the effective thermal conductivity and heat capacity could be regarded as constant during the collapsing process.

Next, we set out to estimate the cell viability ratio under the conditions of the present bio-experimental setup. Given the generation mechanism of the bubbles resulting in the effective activation, the number of the bubbles M_1 for triggering the electric discharge once can be estimated by [46]

$$M_1 = \frac{V_{air}}{V_{bubble}} = \frac{V_{air}}{4/_3 \pi R_0^3}, \tag{21}$$

where V_{air} is the volume of air in the slot of the test chamber, R_0 is the initial bubble radius.

Considering the condition of the cell experiments, the sample extraction was conducted every 20-shot electric discharges. Assuming that the generated bubbles after every electric discharge are accumulated, the total number of the bubbles before the extraction of the sample is presented by

$$M_n = M_1 \sum_{i=1}^{n} i. \tag{22}$$

where n is the number of the electric discharges before the extraction of the sample in the experiments. The average number of the bubble after every electric discharge can be rewritten by

$$M = M_1 \frac{\sum_{i=1}^{n} i}{n} = \frac{V_{air}}{4/_3 \pi R_0^3} \frac{\sum_{i=1}^{n} i}{n}. \tag{23}$$

According to the present experimental system, V_{air} = 3.982 × 10^{-7} m^3, R_0 = 50 μm, V_{bubble} = 5.24 × 10^{-13} m^3, n = 20, V = 12 ml, r_s = 25.78 μm, M = 7.68 × 10^6, and λ_1 = 0.0382 were obtained. Therefore, we attain the viability ratio

ACCEPTED MANUSCRIPT

of marine bacteria, N_t/N_0, when one incident shock wave passes through M of the generated bubbles in the test chamber. However, as shown in Fig. 6, multiple shock waves were produced due to the reflection and concentration in the test chamber. To get close to the real pressure field, a coefficient β is defined as the number of incident shock wave when the electric discharge is triggered once. The Eq. (7) would be changed to Eq. (24).

$$\frac{N_t}{N_0} = e^{-\lambda_1 t} = e^{-\beta\lambda_1 t} \tag{24}$$

Figure 9 shows a comparison in viability ratio of marine bacteria between the bio-experimental results and the estimation of the theoretical model. The open circles indicate the average of 6-set experimental results. The initial density of marine bacteria ranged from 2.62×10^7 cfu/ml to 8.65×10^5 cfu/ml. From the figure, that the viability ratios of marine bacteria are decreasing exponentially, so that a maximum and minimum for the viability ratio are expressed by $y = e^{-0.098t}$ and $y = e^{-0.072t}$, respectively, as indicated by the dashed lines. The solid lines represent the estimation by the theoretical model at $\beta = 1$, 2, and 3, respectively. It can be seen that the experimental data were just between the estimation of $\beta = 1$ and $\beta = 3$. The pressure profile of incident shock wave shown in Fig. 6 was obtained when numerous bubbles were not generated, so that we observed clearly the 2nd shock wave, the concentration of reflected shock waves at the inner wall of the test chamber. However, the motion of numerous bubbles would affect the propagation behaviors of the underwater shock waves. Therefore, the number of incident shock wave β changes between 1 and 3. As a result, the estimation by the theoretical model shows good agreements with the bio-experimental data.

Substituting Eq. (23) into Eq. (2), the inactivation ratio of the cells for a single bubble λ_1 is rewritten by Eq. (25). It is found that the dimensionless radius of the sterilized space, r_s/R_0, determine directly the value of λ_1, and thus the viability ratio of marine bacteria. Figure 10 shows the relationship between initial radius and dimensionless radius of the sterilized space r_s/R_0 for a bubble. From the figure, we could see that the value of the dimensionless radius increases with the initial radius and reaches about 0.5 for a 25 μm radius bubble. The phenomenon is caused due to the respectively large surface tension. After that, the value of r_s/R_0 hardly changes. It indicates that the sizes of the bubbles do not influence the sterilization effect in the case of larger bubbles than 25 μm radius, i.e., the initial radius of bubble is an insensitive factor in estimating the viability ratio of marine bacteria.

$$\lambda_1 = \frac{V_{air}}{V}\frac{\sum_{i=1}^{n} i}{n}\left(\frac{r_s}{R_0}\right)^3 \tag{25}$$

4. Summary

The paper reported on a theoretical model consisting of a biological probability model for cell viability and a bubble dynamic model, to predict the inactivation effects in the interaction of bubbles and underwater shock waves. From the viewpoint of the chemical inactivation, the biological probability model was developed to estimate the viability ratio by defining the sterilized space of the OH radicals. The generation of the OH radicals are related to the temperature inside the bubble. The collapsing motion of bubble was analyzed in the bubble dynamic model based on the Herring equation. Furthermore, the heat conductivity and mass transportation through the boundary layer were considered in the model. In the model, the radius of the sterilized space was defined as the bubble radius when the internal temperature achieved 1000 K, the critical condition for generating the OH radicals.

On the other hand, bio-experiments of marine *Vibrio* sp. were carried out in the test chamber of a cylindrical water chamber. A high voltage power supply was used to generate underwater shock waves. The propagation behaviors were also analyzed by the pressure measurement of a pressure transducer. The bubbles for inducing effective inactivation of marine bacteria were produced by the rapid up-and-down movement of liquid surface in the slot of the test chamber. Here, the ascorbic sodium was added into the cell suspension to remove the inactivation effects of the OH radicals. The bio-experimental results showed that the marine bacteria are killed by the chemical actions of the OH radicals rather than the mechanical of the bubble motion. Furthermore, the viability ratio of marine bacteria decreased exponentially.

For estimating the viability ratio by the theoretical model, we discussed the number of the generated bubbles and pressure waveform they exposed to in consideration of the experimental conditions. Given the results of the pressure measurement, there were more than an incident shock pressure leading to the motion of the bubble after once trigger of the electric discharge. Consequently, the number of incident shock wave was also considered in the theoretical model. As a result, the estimation by the model shows good agreements with the bio-experimental data.

In our previous study, we have investigated the cell damage induced by underwater shock wave via an electron microscope. The deformation obviously differed from that by the osmotic pressure. In order to improve the sterilization effect of marine bacteria, it is necessary to find a method to efficiently generate OH radicals in a simpler way. The size and number density of bubbles, strength and waveform of external introducing pressure to induce

ACCEPTED MANUSCRIPT

bubble motion are important parameters. Identification of optimum conditions for these parameters is required by considering a chemical reaction model. For better understanding the model, it may be interesting to investigate more accurate critical conditions for generating the OH radicals

Acknowledgement

This work was supported by the National Natural Science Foundation of China, grant numbers11802311, 11772340, and 11672315, the Youth Innovation Promotion Association CAS (2015015), and the JSPS KAKENHI, grant Numbers 16H04600 and 16K14512.

Appendix

In the bio-experiments, the underwater electric discharge was used to generate shock waves. During the process of the electric discharge, ultrasound (UV) light was also thought to be emitted. Sun et al. [47] investigated the characteristics of the UV light emitted by the electric discharges. They argued that the energy of the UV light was 3.2 % of the total energy. In other research, UV light has been applied to the sterilization in some fields such as food and marine engineering. Iwaguch et al. [48] constructed a novel microwave-UV light sterilization system and investigated the sterilization effects of the UV light. They pointed out a sterilization effect was clearly obtained using only irradiation with UV light. The experimental result in Ref. [5] also indicates that UV produced by the electric discharges affected the inactivation of *E. coli* in saline solutions. Hence, to examine the sterilization effect of the UV light produced by the underwater electric discharge, we used the experimental arrangement shown in Fig. A.1 in Ref. [49]. The water chamber consisted of two parts, namely, an ellipsoidal chamber in which the underwater electric discharge was triggered and an upper chamber filled with a cell suspension of the marine *Vibrio* sp. A 0.1-mm silicone film was used to separate the two chambers. To prevent the underwater shock waves from the electric discharge propagating into the cell suspension, an air gap of about 5 mm between the water surface and the silicone film was employed to ensure that the cell suspension was irradiated only by UV light, as shown in Fig. A.1 (b).

Fig. A.2 shows an estimation of the number of viable cells under condition 1 (UV light and shock pressure) and condition 2 (UV light only). The solid squares and diamonds represent the bio-experimental results under condition 1 and condition 2, respectively. During the experiments, the applied frequency was 1 Hz and the output power was 31.6 kV. After 200 s, it was found that there had been very little sterilization under condition 2 (UV light only) while about two orders of the marine bacteria were killed by the shock pressure. Therefore, we can say that that the UV light emitted by the electric discharges is ineffective at killing the marine bacteria in the present underwater system.

Reference

[1] K. Takayama, Application of Underwater Shock Wave Focusing to the Development of Extracorporeal Shock Wave Lithotripsy, Japanese Journal of Applied Physics 32 (1993) 2192-2198.

[2] M. Delius, F. Ueberle, W. Eisenmenger, Extracorporeal shock waves act by shock wave-gas bubble interaction, Ultrasound in medicine & biology 24 (1998) 1055-1059.

[3] M. Lokhandwalla, B. Sturtevant, Mechanical haemolysis in shock wave lithotripsy (SWL): I. Analysis of cell deformation due to SWL flow-fields, Physics in medicine and biology 46 (2001) 413-437.

[4] M. Lokhandwalla, J. A. Mcateer, J. C. W. Jr, B. Sturtevant, Mechanical haemolysis in shock wave lithotripsy (SWL): Ⅱ. I*n vitro* cell lysis due to shear, Physics in medicine and biology 46 (2001) 1245-1264.

[5] A. M. Loske, U. M. Alvarez, C. Hernández-Galicia, E. Castaño-Tostado, F. E. Prieto, "Bactericidal effect of underwater shock waves on Escherichia coli ATCC 10536 suspensions, Innovative Food Science & Emerging Technologies 3 (2002) 321-327.

[6] K. Okada, N. Kudo, T. Kondo, K. Yamamoto, Contributions of mechanical and sonochemical effects to cell membrane damage induced by single-shot pulsed ultrasound with adjacent microbubble, Journal of Medical Ultralsonics 35 (2008) 169-176.

[7] A. Abe, H. Mimura, H. Ishida, K. Yoshida, The effect of shock pressures on the inactivation of a marine *Vibrio* sp., Shock Waves 17 (2007) 143-151.

[8] A. Abe, K.Ohtani, K. Takayama, S. Nishio, H. Mimura, M. Takeda, Pressure generation from micro-bubble collapse at shock wave loading, Journal of Fluid Science and Technology 5 (2010) 235-246.

[9] A. Abe, H. Mimura, Sterilization of Ships' Ballast Water, Bubble Dynamics and Shock Waves, Springer Berlin Heidelberg (2013) 339-362.

[10] J. Wang, A. Abe, Experimental Verification of Shock Sterilization for Marine *Vibrio* sp. using Microbubbles Interacting with Underwater Shock Waves, Journal of Marine Science and Technology 21 (2016) 679-688.

[11] J. Wang, A. Abe, Y. Wang, C. Huang, Fundamental study of sterilization effects on marine Vibrio sp. in a cylindrical water chamber with supply of only underwater shock waves, Ultrasonics Sonochemisty 42 (2018) 541-550.

[12] K. Yasui, T. Tuziuti, M. Sivakumar, Y. Iida, Theoretical study of single-bubble Sonochemistry, Journal of Chemical Physics 122 (2005) 224706.

[13] K. Yasui, T. Tuziuti, Y. Iida, H. Mitome, Theoretical study of the ambient-pressure dependence of sonochemical reactions, The Journal of Chemical Physics 119 (2003) 346-356.

ACCEPTED MANUSCRIPT

[14] S. Merouani, O. Hamdaoui, Y. Rezgui, M. Guemini, Theoretical estimation of the temperature and pressure within collapsing acoustical bubbles, Ultrasonics Sonochemistry 21 (2014) 53-59.
[15] S. Merouani, O. Hamdaoui, F. Saoudi, M. Chiha, Sonochemical degradation of Rhodamine B in aqueous phase: Effects of additives, Chemical Engineering Journal 158 (2010) 550-557.
[16] S. Merouani, O. Hamdaoui, F. Saoudi, M. Chiha, Influence of experimental parameters on Sonochemistry dosimetries: KI oxidation, Fricke reaction and H_2O_2 production, Journal of Hazardous Materials 178 (2010) 1007-1014.
[17] K. A. Morch, Cavitation nuclei: experiments and theory, Journal of Hydrodynamics 21 (2009) 176-189.
[18] M. Bai, Z. Zhang, X. Xue, X. Yang, L. Hua, D. Fan, Killing effects of hydroxyl radical on algae and bacteria in ship's ballast water and on their cell morphology, Plasma Chemistry and Plasma Processing 30 (2010) 831-840.
[19] J. Sundaram, B. R. Mellein, S. Mitragotri, An experimental and theoretical analysis of ultrasound-induced permeabilization of cell membranes, Biophysical journal 84 (2003) 3087-3101.
[20] S. Gao, G. D. Lewis, M. Ashokkumar, Y. Hemar, Inactivation of microorganisms by low-frequency high-power ultrasound: 2. A simple model for the inactivation mechanism, Ultrasonics Sonochemisty 21 (2014) 454-460.
[21] J. Wang, A. Abe, A hybrid analytical model of sterilization effect on marine bacteria using microbubbles interacting with shock wave, Journal of Marine Science and Technology 21 (2016) 385-395.
[22] M. P. Brenner, S. Hilgenfeldt, D. Lohse, Single-bubble sonoluminescence, Reviews of Modern Physics 74 (2002) 425-483.
[23] Y. T. Didenko, K. S. Suslick, The energy efficiency of formation of photons, radicals and ions during single-bubble cavitation, Nature 418 (2002) 394-397.
[24] S. Merouani, O. Hamdaoui, Y. Rezgui, M. Guemini, Computer simulation of chemical reactions occurring in collapsing acoustical bubble: dependence of free radicals production on operational conditions, Research on Chemical Intermediates 41 (2015) 881-897.
[25] P. Kanthale, M. Ashokkumar, F. Grieser, Sonoluminescence, sonochemisty (H2O2 yield) and Bubble dynamics: Frequency and power effects, Ultrasonics Sonochemisty 15 (2008) 143-150.
[26] K. Yasui, T. Tuziuti, J. Lee, T. Kozuka, A. Towata, Y. Iida, The range of ambient radius for an active bubble in sonoluminuscence and sonochemical reactions, The Journal of Chemical Physics 128 (2008) 184705.
[27] S. Merouani, O. Hamdaoui, Y. Rezgui, M. Chiha, Sensitivity of free radicals production in acoustically driven bubble to the ultrasonic frequency and nature of dissolved gases, Ultrasonics Sonochemistry 22 (2015) 41-50.
[28] H. Ferkous, S. Merouani, O. Hamdaoui, Y. Rezgui, M. Guemini, Comprehensive experimental and numerical investigations of the effect of frequency and acoustic intensity on the sonolytic degration of napthol blue black in water, Ultrasonics Sonochemistry 26 (2015) 30-39.
[29] S. Merouani, O. Hamdaoui, Z. Boutamine, Y. Rezgui, M. Guemini, Experimental and numerical investigation of the effect of liquid temperature on the sonolytic degradation of some organic dyes in water, Ultrasonics Sonochemisty 28 (2016) 382-392.
[30] M. Takahashi, K. Chiba, P. Li, Free-radical generation from collapsing microbubbles in the absence of a dynamic stimulus, Journal of Physical Chemistry B 111 (2007) 1343-1347.
[31] H. Xu, K. S. Suslick, Molecular emission and temperature measurements from single-bubble sonoluminescence, Physical Review Letters 104 (2010) 1-4.
[32] K. Yasui, T. Tuziuti, Y. Iida, Dependence of the characteristics of bubbles on types of sonochemical reactors, Ultrasonics Sonochemistry 12 (2005) 43-51.
[33] L. Zhang, X. Zhu, H. Yan, Y. Huang, Z. Liu, K. Yan, Luminescence flash and temperature determination of the bubble generated by underwater pulsed discharge, Applied Physics Letters 110 (2017) 034101.
[34] R.J. Locke, K.A. Ockunzzi, OH Imaging In a Lean Burning High-Pressure Combustor, AIAA Journal 34 (1996) 622-624.
[35] B. Varatharajan, F.A. Williams, Chemical-Kinetic Descriptions of High-Temperature Ignition and Detonation of Acetylene-Oxygen-Diluent System, Combustion &Flame 124 (2001) 624-645.
[36] R. Toegel, D. Lohse, Phase diagrams for sonoluminescing bubbles: a comparision between experiment and thoery, Journal of Chemistry Physics 118 (2002) 1863-1875.
[37] C. Herring, Theory of the pulsations of the gas bubble produced by an underwater explosion, Columbia Univ., Division of National Defense Research (1941).
[38] R. Toegel, B. Gompf, R. Pecha, D. Lohse, Does water vapor prevent upscaling sonoluminescence, Physical Review Letters 85 (2000) 3165-3168.
[39] R. Toegel, S. Hilgenfeldt, D. Lohse, Suppressing dissociation in sonoluminescing bubbles: the effect of excluded volume, Physical Review Letter 88 (2002) 034301.
[40] K. Yasui, K. Kato, Bubble dynamics and sonoluminescence from helium and xenon in mercury and water, Physical Review E 86 (2012) 036320.
[41] M. Dular, O. Coutierdelgosha, Thermodynamic effects during growth and collapse of a single cavitation bubble, Journal of Fluid Mechanics 736 (2013) 44-66.

ACCEPTED MANUSCRIPT

ACCEPTED MANUSCRIPT

[42] S. Merouani, H. Ferkous, O. Hamdaoui, Y. Rezgui, M. Guemini, A method for predicting the number of active bubbles in sonochemical reactors, Ultrasonics Sonochemistry 22 (2015) 51-58.
[43] S. Merouani, O. Hamdaoui, Y. Rezgui, M. Guemini, Energy analysis during acoustic bubble oscillations: relationship between bubble energy and sonochemical parameters, Ultrasonics 54 (2014) 227-232.
[44] B.D. Storey, A.J. Szeri, Water vapor, sonoluminescence and sonochemistry, Proceedings of the Royal Society of London A 456 (2000) 1685–1709.
[45] G. Hauke, D. Fuster, C. Dopazo, Dynamic of a single cavitating and reacting bubble, Physical Review E 75 (2007) 066310.
[46] C. Xu, Y. Wang, C. Huang, J. Huang, C. Yu, The effect of free surface on cloud cavitating flow around a blunt body. Journal of Hydrodynamics 29 (2017) 979-986
[47] B. Sun, S. Kunitomo, C. Igarashi, Characteristics of ultraviolet light and radicals formed by pulsed discharge in water, Journal of Physics D: Applied Physics 39 (2006) 3814-3820.
[48] S. Iwaguch, K. Matsumura, Y. Tokuoka, S. Wakui, N. Kawashima, Sterilization system using microwave and UV light, Colloids and Surface B: Biointerfaces 25 (2002) 299-304.
[49] N. Tsujii, B. Wan, H. Mimura, A. Abe, Experimental study on inactivation of marine bacteria using electric discharge shock waves, 28th International Symposium on Shock Waves 2 (2012) 915-921.
Fig. 1 Schematic of experimental setup for estimating sterilization effect
Fig. 2 Colonies of marine *Vibrio* sp. on agar plate
Fig. 3 Schematic of sterilized space of single bubble from test chamber filled with cell suspension
Fig. 4 Schematic of single bubble dynamic model on generation and diffusion of OH radicals: (a) Collapsing motion of bubble induced by incident shock wave, (b) Determination of radius of sterilized space
Fig. 5 Estimation of cell viability at electric discharge of 31.6 kV with air gap of 10 mm in slot of test chamber: ■ with and ◆ without sodium L-ascorbate
Fig. 6 Pressure profile at position of 30 mm from discharge point obtained with FOPH 2000 in test chamber
Fig. 7 Analytical results of bubble motion equation for 50-μm radius bubble after passage of incident shock wave: (a) Time variation of radius and pressure of incident shock wave and (b) Time variation of temperature inside bubble
Fig. 8 Time variations of number of total molecules (blue line) and water vapor (orange line) inside bubble
Fig. 9 Comparison in viability ratio of bacteria between bio-experimental results and estimation of theoretical model
Fig. 10 Relationship between initial radius and dimensionless radius of sterilized space r_s/R_0 around bubble
Fig. A.1 Schematic of experimental setup for determining effect of UV light on cell viability of marine *Vibrio* sp.
Fig. A.2 Estimation of number of viable cells from bio-experiments under condition 1 (flash light and shock pressures) ■, and condition 2 (flash light only) ◆

- A theoretical model is developed to estimate inactivation effects of OH radicals in bubble-shock interaction.
- It consists of a biological probability model for cell viability and a bubble dynamic model for bubble-shock interaction.
- Heat conductivity and mass transportation through a boundary layer are considered in the model.
- The estimation by the model shows good agreements with the bio-experimental data.

ACCEPTED MANUSCRIPT

ACCEPTED MANUSCRIPT

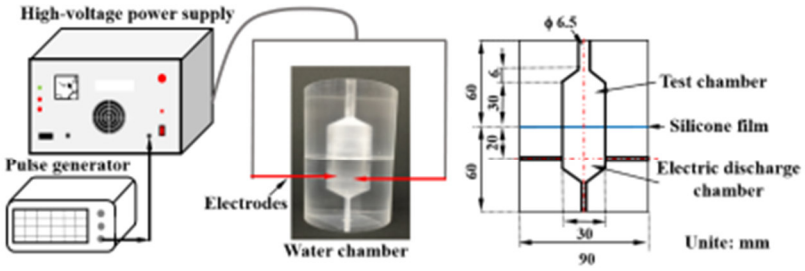

Fig. 1 Schematic of experimental setup for estimating sterilization effect

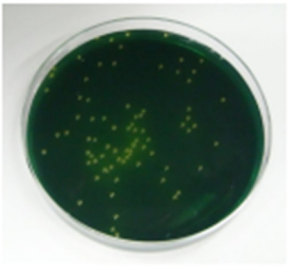

Fig. 2 Colonies of marine *Vibrio* sp. on agar plate

ACCEPTED MANUSCRIPT

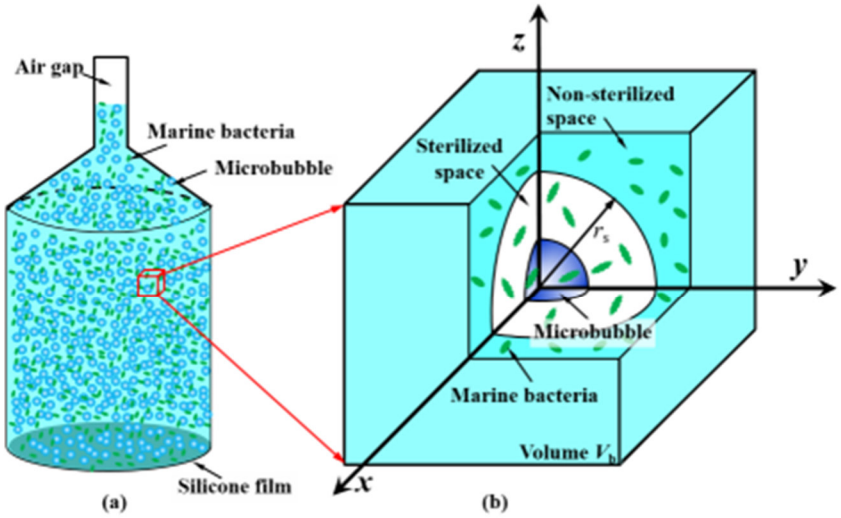

Fig. 3 Schematic of sterilized space of single bubble from test chamber filled with cell suspension

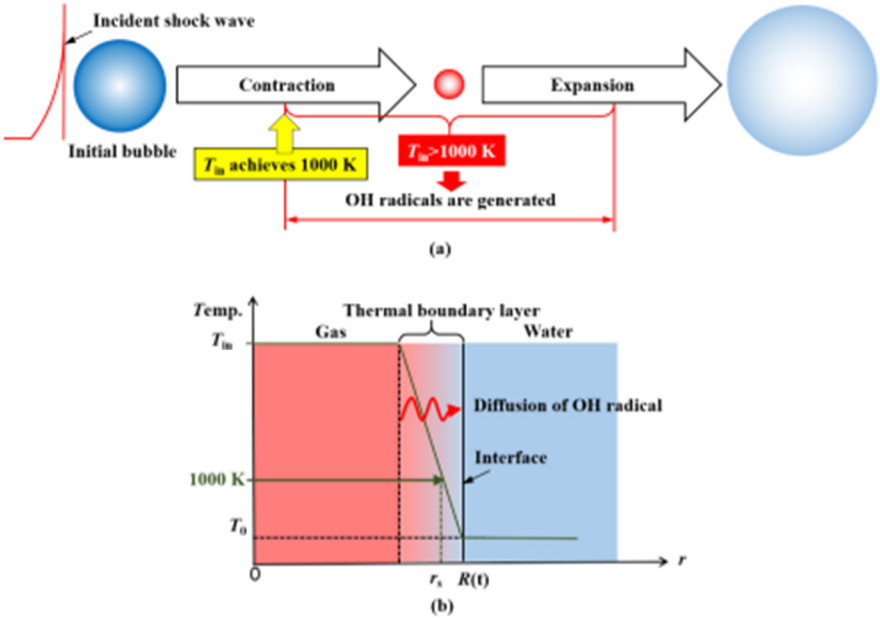

Fig. 4 Schematic of single bubble dynamic model on generation and diffusion of OH radicals: (a) Collapsing motion of bubble induced by incident shock wave, (b) Determination of radius of sterilized space

ACCEPTED MANUSCRIPT

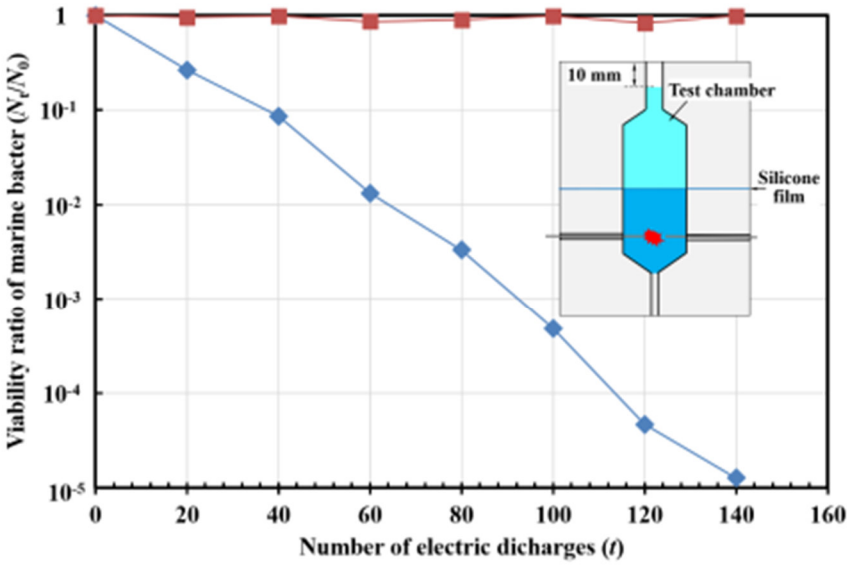

Fig. 5 Estimation of cell viability at electric discharge of 31.6 kV with air gap of 10 mm in slot of test chamber: ■ with and ◆ without sodium L-ascorbate

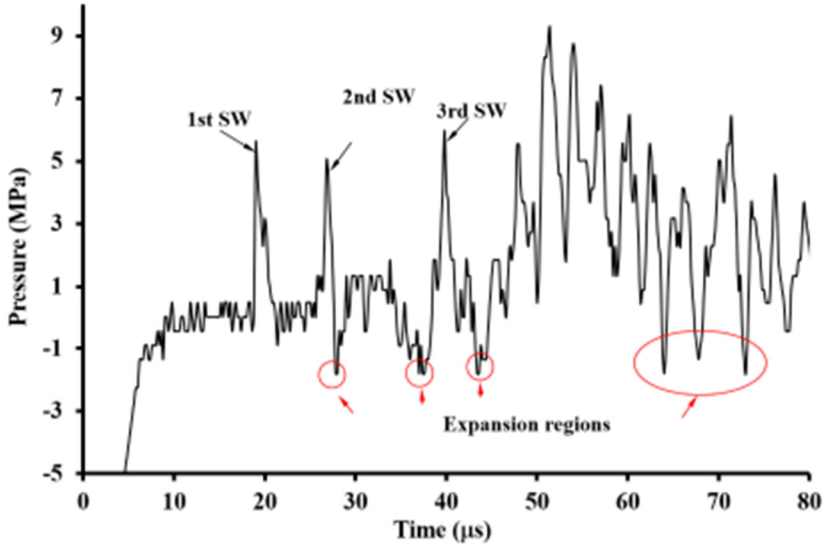

Fig. 6 Pressure profile at position of 30 mm from discharge point obtained with FOPH 2000 in test chamber

ACCEPTED MANUSCRIPT

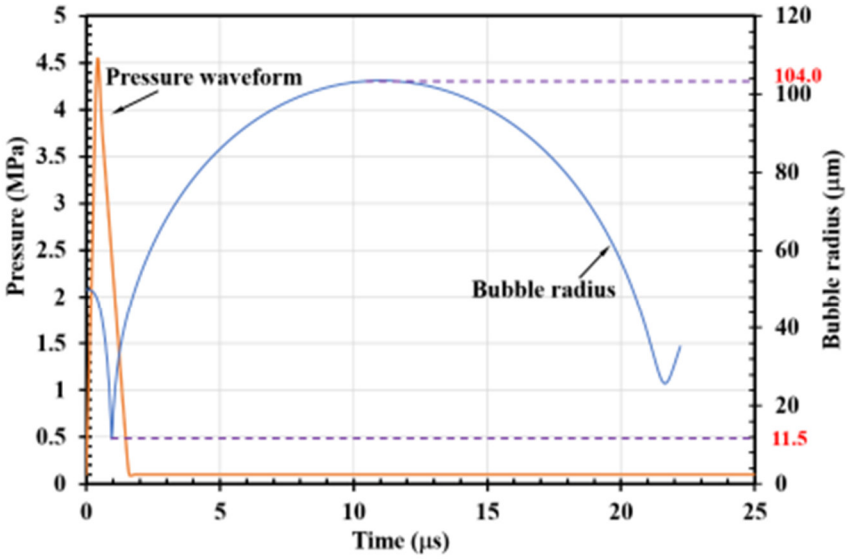

(a) Time variation of radius and pressure of incident shock wave

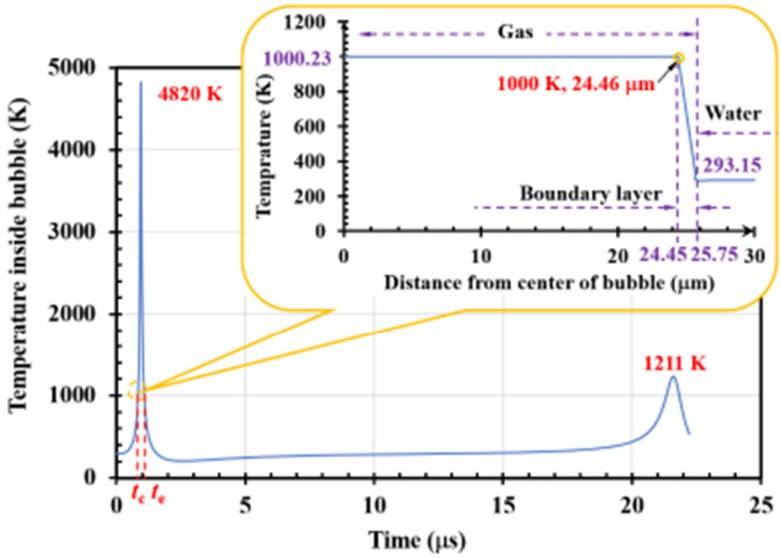

(b) Time variation of temperature inside bubble

Fig. 7 Analytical results of bubble motion equation for 50-μm radius bubble after passage of incident shock wave

ACCEPTED MANUSCRIPT

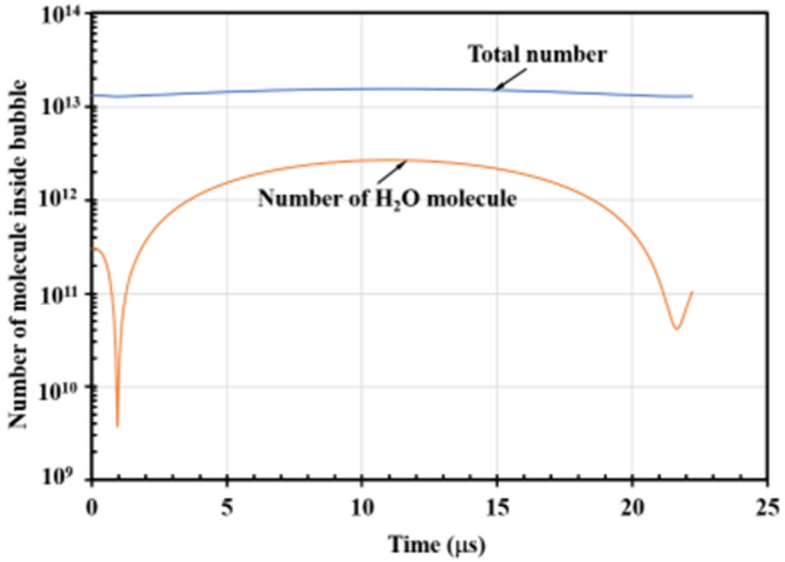

Fig. 8 Time variations of number of total molecules (blue line) and water vapor (orange line) inside bubble

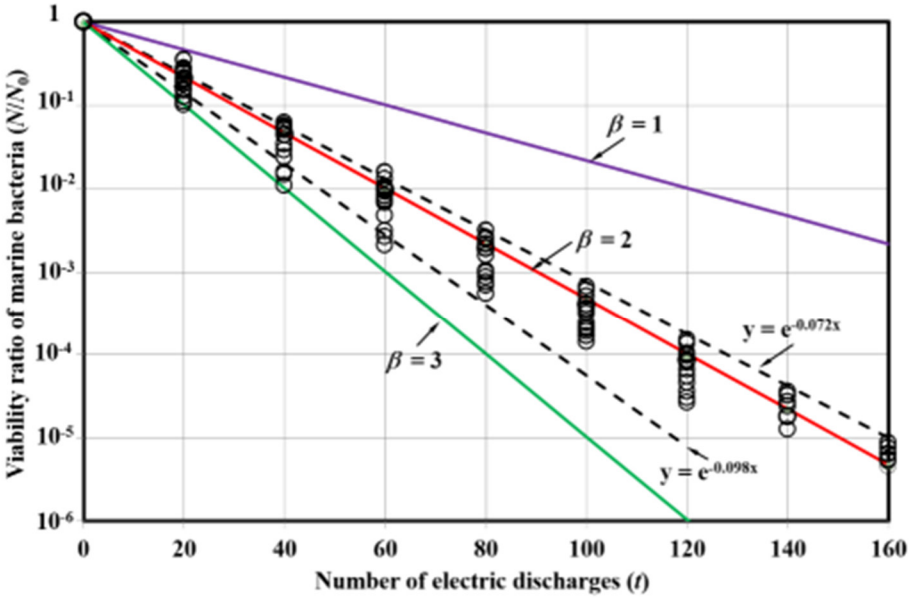

Fig. 9 Comparison in viability ratio of bacteria between bio-experimental results and estimation of theoretical model

ACCEPTED MANUSCRIPT

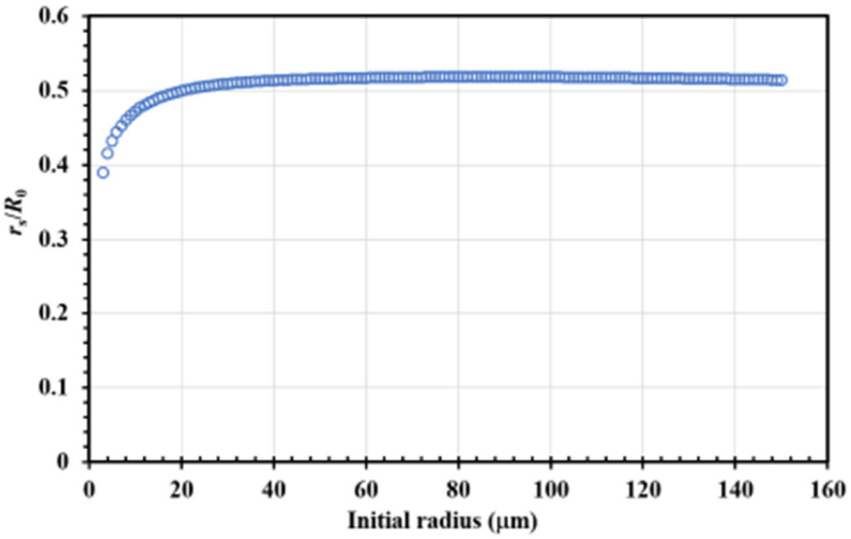

Fig. 10 Relationship between initial radius and dimensionless radius of sterilized space r_s/R_0 around bubble

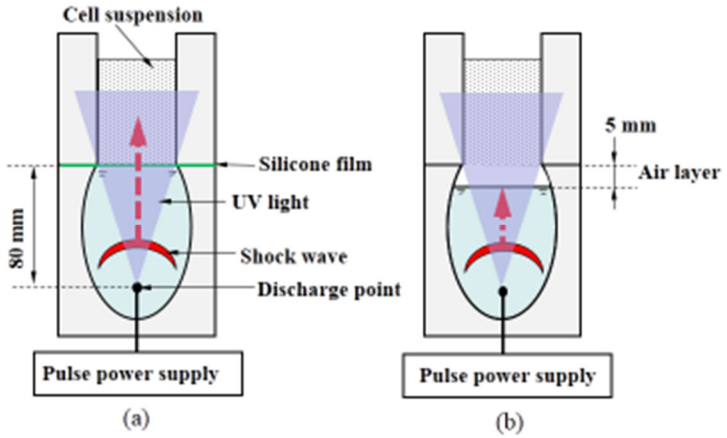

Fig. A.1 Schematic of experimental setup for determining effect of UV light on cell viability of marine *Vibrio* sp.

ACCEPTED MANUSCRIPT

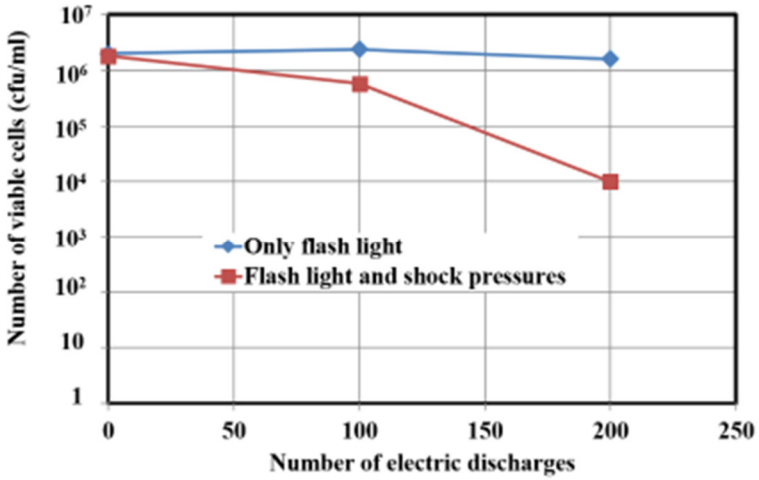

Fig. A.2 Estimation of number of viable cells from bio-experiments under condition 1 (flash light and shock pressures) ■, and condition 2 (flash light only) ◆

ACCEPTED MANUSCRIPT